J Ther Eng, Vol. 7, Supp 14, pp. 2041–2053, December 2021

Journal of Thermal Engineering
Web page info: https://jten.yildiz.edu.tr
DOI: 10.18186/thermal.1051307

Journal of Thermal Engineering

Research Article

Investigation of laminar forced convection heat transfer of nanofluids through flat plate solar collector

Farzad HOSSAIN[1]*, Ashrafuzzaman MIAH[1], Afshana MORSHED[2], Insiat Islam RABBY[3], Eric HU[4]

[1]*Department of Mechanical and Production Engineering, Islamic University of Technology, Boardbazar, Gazipur-1704, Bangladesh*

[2]*School of Mechanical, Materials & Mechatronic Engineering, University of Wollongong, Wollongong, New South Wales, Australia*

[3]*Department of Mechanical and Manufacturing Engineering, Universiti Putra Malaysia, Seri Kembangan, Selangor, Malaysia*

[4]*Department of Mechanical Engineering, University of Adelaide, North Terrace, Adelaide, SA 5005, Australia*

ARTICLE INFO

Article history
Received: 09 June 2020
Accepted: 21 July 2020

Keywords:
Heat Transfer, Nanofluid, Nanoparticle, Forced Convection, Solar Collector, Flat Plate

ABSTRACT

The paper analyzes laminar forced convection heat transfer for both single and mixture phase models utilizing Al_2O_3-water and CuO-water nanofluids as the working fluid and examines the effect of internal fins in the collector tubes in order to improve collector efficiency. A physical model with governing equations has been defined. Finite volume method has been utilized for discretizing governing equations and finite element method has been utilized for three-dimensional analysis of solar plate model with finned tubes. Convective heat transfer coefficient, Nusselt number and shear stress have been analyzed for Reynolds numbers from 200 to 700 with 0-5% volume fractions of nanofluid. Moreover, the efficiency of the collector has been investigated for constant flow rates from 0.02 to 0.04 mL/s and variable overall heat loss coefficient for the same range of volume fractions of nanofluid. It has been found that increment of shear stress and heat transfer coefficient occurred with the increment of concentration of nanoparticles and the Reynolds number. Investigation of particle size has not shown any notable variation with the mixture phase model. Mixture-phase model gives comparatively lower values due to the reduction of viscosity near the wall. Noticeable increment of efficiency has been observed by changing working fluid from Al_2O_3-water to CuO-water which has been further improved by utilizing variable overall heat loss coefficient. Efficiency increases up to 6.5% and 8.7% than the base fluid for utilizing Al_2O_3-water and CuO-water nanofluid respectively. Additionally, utilizing internal fins to the riser tubes, the efficiency increases up to 11%.

Cite this article as: Farzad H, Md. Ashrafuzzaman M, Afshana M, Md Insiat I R, Eric H. Investigation of laminar forced convection heat transfer of nanofluids through flat plate solar collector. J Ther Eng 2021;7(Supp 14):2041–2053.

***Corresponding author.**
*E-mail address: farzadhossain@iut-dhaka.edu

This paper was recommended for publication in revised form by Regional editor Tolga Taner

Published by Yıldız Technical University Press, İstanbul, Turkey

INTRODUCTION

The solar collector is basically a heat device that collects solar radiation and supply to useful applications. Nowadays, flat plate solar collector is utilized all over the world due to its various advantages. However, conventional solar collectors cannot facilitate such advantages. Nanofluid is one of today's innovative technologies. Nanofluid is basically a combination of low-thermal conductive base fluid and high-thermal conductive nano sized solid particles, which affects the thermophysical characteristics of the base fluid [1]. Owing to its high heat transfer properties, nanofluid offers a better performance in heat exchangers than the base fluid. In addition, nanofluid requires less energy to achieve the same amount of heat transfer because of the less energy needed for pumping than the base fluid. Therefore, utilizing nanofluids in place of conventional fluid can increase efficiency.

Choi and Eastman [2] suggested nanofluid for the first time and they found that utilizing nanofluid can significantly increase thermal conductivity. Agarwal et al. [3] observed that nanofluids were shown to be very stable in lower volume fractions compared with the higher volume fraction. The utilization of nanofluids will remarkably raise the heat transfer coefficient, while at the same time, dramatically increase thermal conductivity, viscosity, particle size and particle concentration [4-10]. Moreover, energy is an important topic, and effective utilization of energy can reduce environmental emissions [11]. Harvesting solar energy has become a very important phenomenon in recent years [12]. Though flat plate solar collector has low efficiency in comparison to other types of solar collector, still it is utilized nowadays because of its low cost and high durability and reliability. Meanwhile, metal heat pipes, as well as internal fins, have been utilized for enhancing solar collectors' performance [13, 14]. Furthermore, thermal performance has been raised considerably by the utilization of nanofluids in the flat plate collector [15, 16].

Tiwari et al. [17] investigated active solar distillation method of flat plate collector and found that their proposed model can meet not only the daily potable water's demand but also the DC electricity in sunshine hours. Verma et al. [18] worked with flat plate solar collector utilizing various nanofluids and found minimum entropy generation and maximum energy efficiency with Multiwalled carbon nanotube/water. Genc et al. [19] observed transient behavior of flat plate collector and identified the growth of thermal efficiency utilizing nanofluid for lower flow rates. Hawwash et al. [20] worked with various types of working fluids and found the increment of FPCS thermal efficiency by utilizing Alumina nanofluid up to 0.5% volume fraction. Mahbubul et al. [21] worked with carbon nanotube nanofluid and observed around 10% higher efficiency than water utilizing 0.2% nanofluid in the solar collector. Kiliç et al. [22] worked with titanium dioxide/water nanofluid and observed more than 12% efficiency increment by utilizing nanofluid instead of pure water. Khan et al. [23] reviewed solar collectors and found higher efficiency in the flat plate water heating collectors in comparison to the air heating collectors. Pandey and Chaurasiya [24] reviewed flat plate solar collector in order to find appropriate techniques for improving efficiency.

Hussein [25] reviewed the application of nanotechnology in renewable energy and found a significant bridge between renewable energy and nanotechnology. Hussein and Walunj [26] found a remarkable increase of direct absorption type solar collectors' performance by utilizing nanofluids. Li et al. [27] identified that the thermal performance of phase change material filled double-glazed units has been enhanced whenever latent heat, density and melting temperatures are increased. Moreover, the utilization of nanofluid has a significant impact in case of efficiency improvement of solar collectors [28, 29]. Chand et al. [30] identified destabilizing effects by using Darcy and Prandtl numbers and stabilizing effects by utilizing modified diffusivity ratio and Lewis number. Kareem et al. [31] found the highest amount of Nusselt number by utilizing SiO_2–water nanofluid. Kamel et al. [32] and Al-Rashed et al. [33] also found significant improvement by the utilization of nanofluid. Mehryan et al. [34] fixed various inclination angles at various locations in order to explore the heat transfer and discovered that the inclination angles and the heat transfer have been significantly affected by the position of the fixed points. Yarmohammadi et al. [35] found the enhancement of heat transfer coefficient and pressure drop by utilizing corrugated tubes. Among the observed metal oxides, utilizing CuO-water nanofluid can improve the highest amount of efficiency of a flat plate solar collector [36, 37]. Sharafeldin and Gróf [38] carried out an investigation by utilizing CeO_2-water nanofluid and identified that the efficiency of the collector had been increased up to 10.74%. Jouybari et al. [39] examined that SiO_2 nanofluid has a significant impact on efficiency in spite of having low thermal conductivity. Farshad et al. [40] found a proportional relationship between thermal performance and geometric variables. Akram et al. [41] identified that thermophysical properties were negatively affected for utilizing surfactants and thermal efficiency was positively influenced for using optimum values of particle size. Tong et al. [42] investigated thermal efficiency of solar collectors and found the efficiency increment of 16% and 21% by utilizing CuO and Al_2O_3 nanofluid respectively. Dutta and Kundu [43] and Roy et al. [44] also investigated thermal performance of flat plate solar collectors by utilizing nanofluid.

Though there are a number of papers in flat plate solar collectors, the majority of them analyzed utilizing only one nanofluid and very few papers investigated both single and mixture phase models at the same time. The paper analyzes laminar forced convection heat transfer for both single and mixture phase models utilizing not only Al_2O_3-water

nanofluid but also CuO-water nanofluid. Moreover, the effect of internal fins in the collector tubes has been examined in order to improve collector efficiency. So, the paper has presented a wide variety of analyses for the two nanofluids to enhance the collector efficiency which is rare in the literature. In addition, the obtained results can be compared with each other. So, it fulfills the gaps and helps researchers to do further research in the future. The result obtained from this paper can also be utilized for developing effective models.

PHYSICAL MODEL

A straight circular pipe of radius 7.2 mm and length 1.6 m have been considered. Assuming the solution is dilute and the fluid (water) flow has been considered steady-state and incompressible. Moreover, the three-dimensional pipe is transformed into a two-dimensional rectangular domain due to axi-symmetric study. Figure 1 represents rectangular domain for the study of nanofluid.

Now, a copper absorber plate of length 1.6 m and width 1.28 m with eight copper riser tubes have been considered. Eight identical parts have been made from the absorber plate with one riser tube in each part. Each of the parts is 0.16 m width. Due to this type of division, every part maintained the same temperature profiles and fluid flows. Figure 2 represents isometric view of flat plate collector model considering one part from the identical parts.

Moreover, internally finned tubes have been utilized in order to enhance the heat transfer between the fluid and the pipe. Two types of fins have been shown in Figure 3 (a) and 3 (b). Isosceles triangular shaped fin-1 has been circumferentially arranged to the inner surface of the pipe. On the contrary, rectangular shaped fin-2 has been diagonally arranged such that they can equally divide the cross section of the pipe.

Table 1. represents parameters considered in the study.

Copper has been chosen as material due to its high thermal conductivity and corrosion resistance. High transparent glass cover has been chosen in order to get enough sunlight. Anti-reflective glass cover has been chosen in order to reduce reflections and increase transmission of light so that more electricity can be generated. The expected life of the flat plate collector is 28 years, and the approximate payback period is 7.5 years. Moreover, it has the ability to utilize in the residential system, around 70 gallons per day.

MATHEMATICAL MODEL

Governing Equations

The governing equations utilized in the paper can be written as follows:

Continuity equation for steady-state and incompressible flow [45],

$$\nabla.(u) = 0 \tag{1}$$

Continuity equation in cylindrical coordinates for steady-state and incompressible flow [46],

$$\frac{1}{r}\frac{\partial(ru_r)}{\partial r} + \frac{1}{r}\frac{\partial(u_\theta)}{\partial \theta} + \frac{\partial u_z}{\partial z} = 0 \tag{2}$$

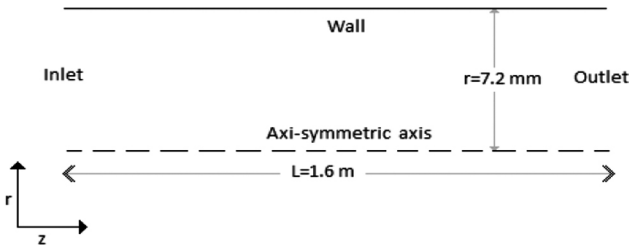

Figure 1. Rectangular domain for study of nanofluid.

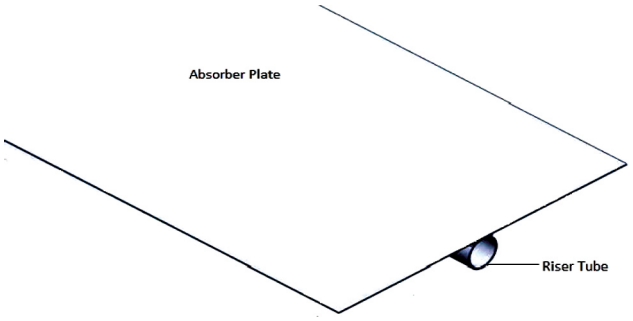

Figure 2. Isometric view of flat plate collector model.

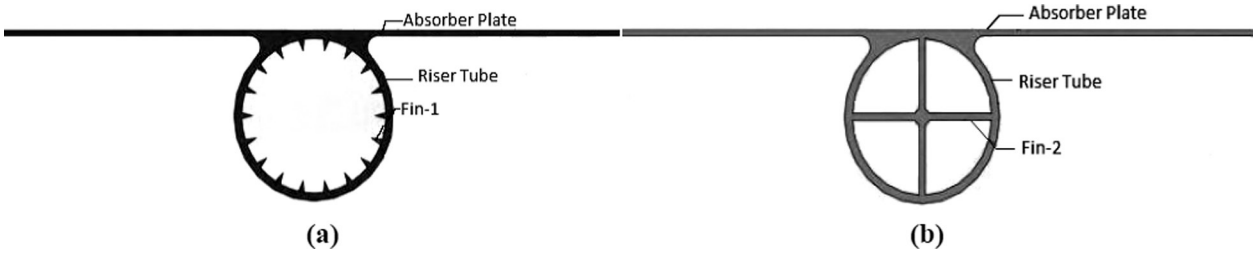

Figure 3. Configuration of (a) Fin-1, (b) Fin-2.

Nanoparticle continuity equation for steady-state and incompressible flow [47],

$$u.\nabla\varphi=\nabla.\left[D_B\nabla_\varphi+D_T\frac{\nabla T}{T}\right] \tag{3}$$

Neglecting source term, *r*-momentum equation for steady-state and incompressible flow [48],

$$\rho\left(u_r\frac{\partial u_r}{\partial r}+\frac{u_\theta}{r}\frac{\partial u_r}{\partial\theta}-\frac{u_\theta^2}{r}+u_z\frac{\partial u_r}{\partial z}\right)=-\frac{\partial\rho}{\partial r}+\mu\left[\frac{\partial}{\partial r}\left(\frac{1}{r}\frac{\partial}{\partial r}(ru_r)\right)+\frac{1}{r^2}\frac{\partial^2u_r}{\partial\theta^2}-\frac{2}{r^2}\frac{\partial u_\theta}{\partial\theta}+\frac{\partial^2u_r}{\partial z^2}\right] \tag{4}$$

Neglecting source term, θ-momentum equation for steady-state and incompressible flow [48],

$$\rho\left(u_r\frac{\partial u_\theta}{\partial r}+\frac{u_\theta}{r}\frac{\partial u_\theta}{\partial\theta}-\frac{u_ru_\theta}{r}+u_z\frac{\partial u_\theta}{\partial z}\right)=-\frac{1}{r}\frac{\partial\rho}{\partial\theta}+\mu\left[\frac{\partial}{\partial r}\left(\frac{1}{r}\frac{\partial}{\partial r}(ru_\theta)\right)+\frac{1}{r^2}\frac{\partial^2u_\theta}{\partial\theta^2}+\frac{2}{r^2}\frac{\partial u_r}{\partial\theta}+\frac{\partial^2u_\theta}{\partial z^2}\right] \tag{5}$$

Neglecting source term, z-momentum equation for steady-state and incompressible flow [48],

$$\rho\left(u_r\frac{\partial u_z}{\partial r}+\frac{u_\theta}{r}\frac{\partial u_z}{\partial\theta}+u_z\frac{\partial u_z}{\partial z}\right)=-\frac{\partial\rho}{\partial z}+\mu\left[\frac{1}{r}\frac{\partial}{\partial r}\left(r\frac{\partial u_z}{\partial r}\right)+\frac{1}{r^2}\frac{\partial^2u_z}{\partial\theta^2}+\frac{\partial^2u_z}{\partial z^2}\right] \tag{6}$$

Neglecting source term, energy equation for steady-state and incompressible flow [49],

$$\rho C_p\left[u.\nabla T\right]=k\nabla^2T \tag{7}$$

Here,

$$u.\nabla T=\frac{\partial}{\partial r}(u_rT)+\frac{\partial}{\partial\theta}(u_\theta T)+\frac{\partial}{\partial z}(u_zT) \tag{8}$$

$$\nabla^2T=\frac{\partial}{\partial r}\left(\frac{\partial T}{\partial r}\right)+\frac{\partial}{\partial\theta}\left(\frac{\partial T}{\partial\theta}\right)+\frac{\partial}{\partial z}\left(\frac{\partial T}{\partial z}\right) \tag{9}$$

Conduction heat transfer at steady-state condition [50],

$$k\nabla^2T+S=0 \tag{10}$$

Overall heat loss coefficient [51],

$$U_L=U_t+U_b+U_e \tag{11}$$

Single Phase Model

Here, fluid flow and heat transfer have been considered axi-symmetric that means no change in θ direction. Now, continuity, momentum and energy equation for steady-state and incompressible flow:

Continuity equation,

$$\frac{1}{r}\frac{\partial(ru_r)}{\partial r}+\frac{\partial u_z}{\partial z}=0 \tag{12}$$

Momentum equation:

r-momentum,

$$\rho\left(\frac{1}{r}\frac{\partial}{\partial r}(ru_ru_r)+\frac{\partial}{\partial z}(u_zu_r)\right)=-\frac{\partial\rho}{\partial r}+\mu\left[\frac{\partial}{\partial r}\left(\frac{1}{r}\frac{\partial}{\partial r}(ru_r)\right)+\frac{\partial^2u_r}{\partial z^2}\right] \tag{13}$$

z-momentum,

$$\rho\left(\frac{1}{r}\frac{\partial}{\partial r}(ru_ru_z)+\frac{\partial}{\partial z}(u_zu_z)\right)=-\frac{\partial\rho}{\partial z}+\mu\left[\frac{1}{r}\frac{\partial}{\partial r}\left(r\frac{\partial u_z}{\partial r}\right)+\frac{\partial^2u_z}{\partial z^2}\right] \tag{14}$$

Energy equation,

$$\rho c_p\left[\frac{1}{r}\frac{\partial}{\partial r}(ru_rT)+\frac{\partial}{\partial z}(u_zT)\right]=k\left[\frac{1}{r}\frac{\partial}{\partial r}\left(r\frac{\partial T}{\partial r}\right)+\frac{\partial^2T}{\partial z^2}\right] \tag{15}$$

Mixture Phase Model

Here, assuming axi-symmetric condition and based on Buongiorno [47] model, continuity, momentum and energy equation for steady-state and incompressible flow:

Continuity equation,

$$\frac{1}{r}\frac{\partial}{\partial r}(ru_r\varphi)+\frac{\partial}{\partial z}(u_z\varphi)=\left[\frac{1}{r}\frac{\partial}{\partial r}\left(rD_B\frac{\partial\varphi}{\partial r}\right)+\frac{\partial}{\partial z}\left(D_B\frac{\partial\varphi}{\partial z}\right)\right]+\left[\frac{1}{r}\frac{\partial}{\partial r}\left(r\frac{D_T}{T}\frac{\partial T}{\partial r}\right)+\frac{\partial}{\partial z}\left(\frac{D_T}{T}\frac{\partial T}{\partial z}\right)\right] \tag{16}$$

Momentum equation of mixture phase model is same as single phase model.

Energy equation,

$$\rho c_p\left[\frac{1}{r}\frac{\partial}{\partial r}(ru_rT)+\frac{\partial}{\partial z}(u_zT)\right]=k\left[\frac{1}{r}\frac{\partial}{\partial r}\left(r\frac{\partial T}{\partial r}\right)+\frac{\partial^2T}{\partial z^2}\right]+\rho_{np}\mu\left[D_B\left(r\frac{\partial\varphi}{\partial r}\frac{\partial T}{\partial r}+\frac{\partial\varphi}{\partial z}\frac{\partial T}{\partial z}\right)+\frac{D_T}{T}\left(\frac{\partial T}{\partial r}\frac{\partial T}{\partial r}+\frac{\partial T}{\partial z}\frac{\partial T}{\partial z}\right)\right] \tag{17}$$

Absorber plate

Additional conduction equation,

$$k\left[\frac{\partial T^2}{\partial y^2}+\frac{\partial T^2}{\partial z^2}\right]+\frac{I_t(\tau\alpha)}{t}-\frac{U_L\left(T-T_\alpha\right)}{t}=0 \qquad (18)$$

Finned tube

For finned tube (S=0). So,

$$k\nabla^2 T=0 \qquad (19)$$

Nusselt number and efficiency

Mean Nusselt number [52],

$$Nu_{av}=\frac{h_{av}D}{k} \qquad (20)$$

Efficiency of flat plat collector is the ratio of the useful energy output from a collector, q_u and the total energy fallen on the collector plate, A_cI_t.

Efficiency of flat plat solar collector [53],

$$\eta=\frac{q_u}{A_cI_t} \qquad (21)$$

Here, the useful energy output from the collector [53],

$$q_u=A_c\left[I_t(\tau\alpha)-U_L\left(T_p-T_\alpha\right)\right]=mc_p\left(T_{in}-T_{out}\right) \qquad (22)$$

BOUNDARY CONDITIONS

For the nanofluid model, the investigation of the collector was done by utilizing both single and mixture phase models. Pressure and flow velocity were considered zero at the outlet and the riser wall respectively. Additionally, no heat flux was considered at the absorber side walls.

However, three-dimensional investigation was required for flat plate model with internal fins in the collector tubes. Though pressure and flow velocity were considered same as the nanofluid model, this time no heat flux was considered at the bottom and the absorber side walls. Moreover, insulation was present in the outer part of pipe and bonding.

THERMO-PHYSICAL PROPERTIES OF NANOFLUID

Determining thermo-physical properties of nanofluid are essential because results of computational analysis are depended on them. Such properties include dynamic viscosity, thermal conductivity, density, specific heat. The thermo-physical properties utilized in the paper have been written as follows:

Dynamic viscosity: Nguyen et al. [54] equation has been utilized in order to calculate dynamic viscosity for Al_2O_3-water and CuO-water.

For Al_2O_3-water:

$$\mu_{nf}=0.9e^{14.8\varphi}\mu_{bf} \qquad (23)$$

For CuO-water:

$$\mu_{nf}=\mu_{bf}\left(1.48-31.9\varphi+510\varphi^2+9000\varphi^3\right) \qquad (24)$$

Thermal conductivity: For calculating thermal conductivity, we utilized Pak and Cho [55] equation for Al_2O_3-water and Eastman et al. [56] CuO-water.

For Al_2O_3-water:

$$k_{nf}=k_{bf}\left(1+7.47\varphi\right) \qquad (25)$$

For CuO-water:

$$k_{nf}=k_{bf}\left(1+11.9\varphi\right) \qquad (26)$$

Density: For calculating density, Xuan and Roetzel [57] equation has been utilized.

$$\rho_{nf}=\rho_{np}\varphi+\rho_{bf}\left(1+\varphi\right) \qquad (27)$$

Specific heat: Pak and Cho [55] equation has been utilized in order to calculate specific heat.

For CuO-water:

$$c_{nf}=\left(1-\varphi\right)c_b+\varphi c_p \qquad (28)$$

MESH GENERATION

In the nanofluid study, the three-dimensional domain is transformed into a two-dimensional rectangular domain which is further divided into various small cells or volumes known as meshing. Mesh domain of nanofluid study is shown in Figure 4. In the flat plate collector model with internal fins, three-dimensional investigation is required. Half body is considered due to the symmetric body. Solar

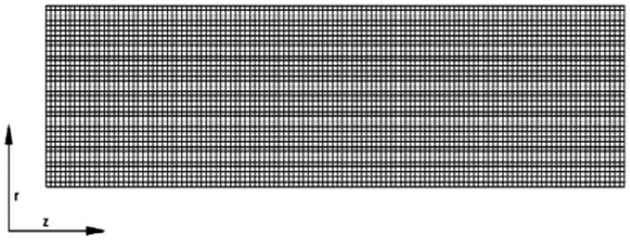

Figure 4. Mesh domain of nanofluid study.

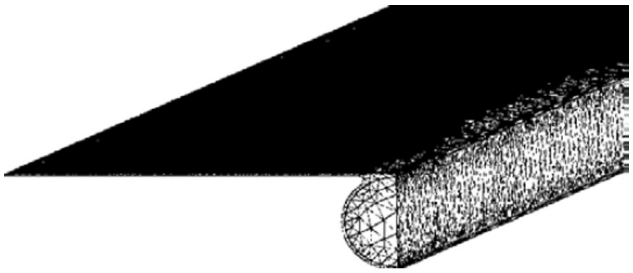

Figure 5.Solar plate domain with mesh

Figure 5. Solar plate domain with mesh.

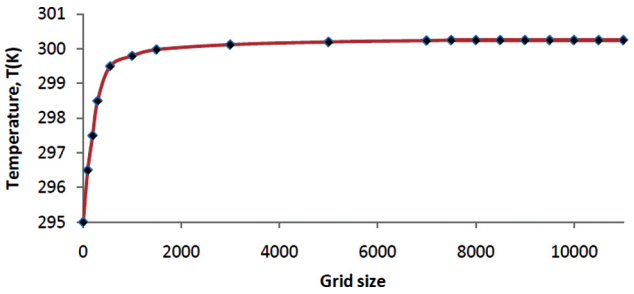

Figure 6 (a). Variation of temperatures for various grid sizes for finite volume method.

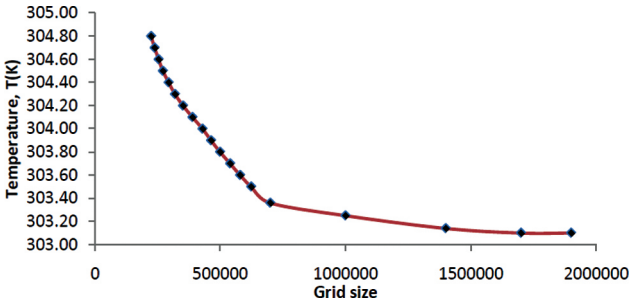

Figure 6 (b). Variation of temperatures for various grid sizes for finite element method.

plate domain with tetrahedral mesh has been shown in Figure 5.

GRID INDEPENDENCE TEST

The grid independence test has been performed with a Reynolds number of 600 and water has been considered as working fluid.

For discretizing the domain, rectangular grids have been utilized. Figure 6 (a) represents variation of temperatures for various grid sizes for finite volume method. Actually, the temperature variation is very small from 1500 grid size. For 1500 grid size, the temperature is 299.98 K which becomes 300.244 K for 7500 grid size. At 8000 grid size, the temperature is around 300.245 K. From 8000 to 11000 grid size, the temperature varies around 0.0000001, which is very small amount of variation. That's why 8000 grid size has been considered satisfactory.

Figure 6 (b) represents variation of temperatures for various grid sizes for finite element method and the investigation of 3D has been done by doing so. From the relationship between the number of grid size and temperature, very little change of temperature has been observed after 1700000 grid sizes and so, it has been considered satisfactory. The difference in the measured temperatures for the last two grid size is around 0.000002. However, after 1900000, grid size could not be computed due to the memory related problem of computer.

CODE VALIDATION TEST

In case of nanofluid study, a code has been written utilizing the finite volume method. The validation has been done by comparing between the Nusselt number correlation obtained from Shah and London [58] equation for constant wall heat flux and the calculated Nusselt numbers for pure water. The validation of code for the study of nanofluid has been represented by Figure 7 (a) which shows almost identical results. Moreover, the calculated Nusselt numbers for pure water are comparatively higher than the correlation results in the developing flow region which gradually reduces and becomes comparatively lower than the correlation results in the fully developed region. The maximum difference between the calculated Nusselt Number and the Nusselt number correlation obtained from Shah and London [58] is 0.0012.

Again, for validating the codes of solar plate study, a comparison has been made among the efficiency obtained from Kalogirou [59] equation and the efficiency obtained for flat plate solar collector by utilizing both FVM and FEM methods. Overall heat loss coefficient, water velocity and atmospheric temperature have been considered as 8 W/m^{2}K, 0.08 m/s and 15°C respectively. The validation of code for the study of solar plate has been represented by Figure 7 (b) which shows nearly similar results. The results obtained from FEM method are marginally lower than the results obtained from FVM method. The maximum difference among the efficiency obtained from Kalogirou [59] equation and the efficiency obtained for flat plate solar collector by utilizing both FVM and FEM methods is 0.017.

The Shah and London correlation is given as follows:

$$Nu_{z_*} = 3.302 z_*^{-\frac{1}{3}} - 1.00;\ z_* \le 0.00005 \tag{29}$$

$$Nu_{z_*} = 1.302 z_*^{-\frac{1}{3}} - 0.50;\ 0.00005 < z_* \le 0.0015 \tag{30}$$

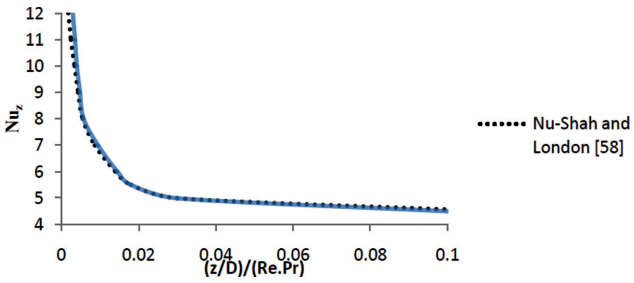

Figure 7 (a). Validation of code for the study of nanofluid.

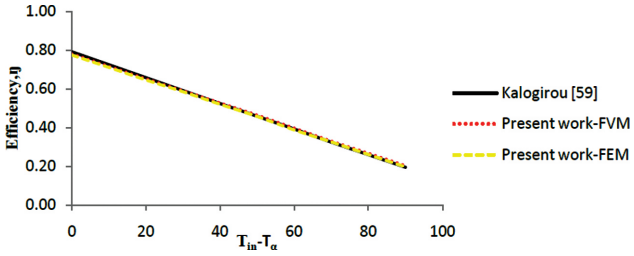

Figure 7 (b). Validation of code for the study of solar plate.

$$Nu_{z_*} = 4.364 + 8.68\left(10^3 z_*\right)^{-0.506} e^{-41 z_*};\ z_* > 0.0015 \quad (31)$$

where

$$z_* = \frac{\frac{Z}{D}}{Re.Pr} \quad (32)$$

RESULTS AND DISCUSSION

Here, nanofluids in a small volume fraction (up to 5%) with Reynolds number from 200 to 700 have been utilized with a constant heat flux of 2400 W/m^2 in order to see the effects of various parameters.

Average convective heat transfer coefficient for various volume fractions of nanoparticle at different Reynolds numbers has been shown in Figure 8 which shows the increment of convective heat transfer coefficient with the increment of Reynolds number and volume fractions of nanoparticle. At a specific volume fraction of nanofluid, single phase model has comparatively higher convective heat transfer coefficient than mixture phase model. At 5% volume fraction of nanofluid, the highest difference of convective heat transfer coefficient between the models has been observed. Almost 36% increment of convective heat transfer coefficient has been observed for 5% volume fraction of nanofluid by utilizing single phase model.

Average Nusselt number for various volume fractions of nanoparticle at different Reynolds numbers has been shown in Figure 9 which shows a small variation of average

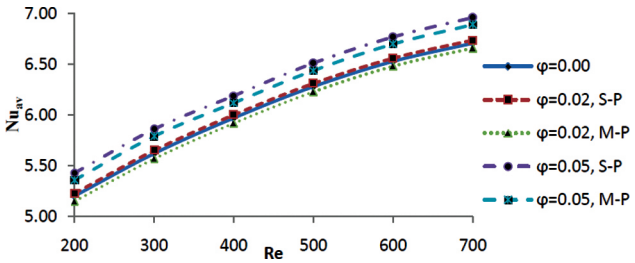

Figure 8. Average convective heat transfer coefficient for various volume fractions of nanoparticle at different Reynolds number.

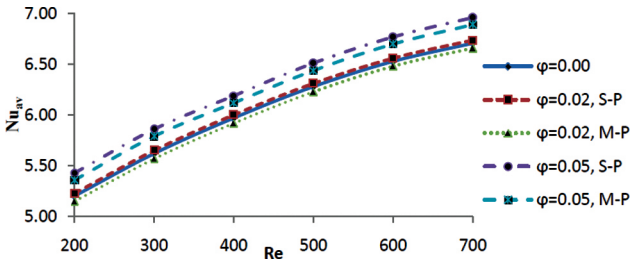

Figure 9. Average Nusselt number for various volume fractions of nanoparticle at different Reynolds number.

Nusselt number with the increment of volume fractions of nanoparticle. At a specific volume fraction of nanofluid, single phase model has comparatively higher average Nusselt number than mixture phase model. At 5% volume fraction of nanofluid, the highest difference of average Nusselt number between the models has been observed. Another noticeable thing is that for lower volume fraction (i.e. 2%) of nanoparticle, average Nusselt number is a little bit higher than water for single phase model whereas average Nusselt number is slightly lower than water for mixture-phase model. The highest increment of average Nusselt number has been observed for 5% volume fraction of nanofluid for both models.

Average shear stress for various volume fractions of nanoparticle at different Reynolds numbers has been shown in Figure 10 which shows the increment of average shear stress is nearly constant with the increment of Reynolds number. The highest increment of average shear stress has been observed for 5% volume fraction of nanofluid for both models which are around 196% and 180% more than water for single phase and mixture phase model respectively.

Average convective heat transfer coefficients for different nanoparticle sizes have been shown in Figure 11 which exhibits sensitivity of particle diameter for mixture-phase model. The average heat transfer coefficient reduces very small with the increment of nanoparticle diameter. It also clearly indicates that the heat transfer coefficient is not

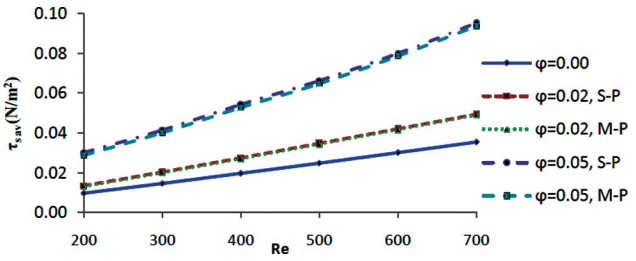

Figure 10. Average shear stress for various volume fractions of nanoparticle at different Reynolds number.

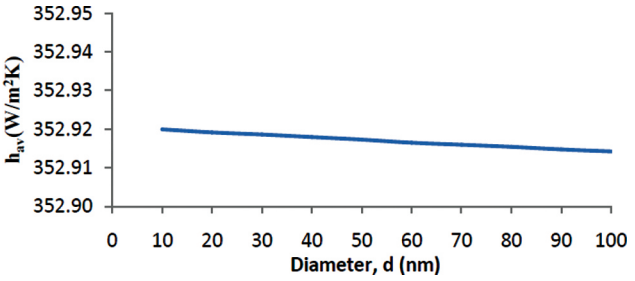

Figure 11. Average convective heat transfer coefficients for different nanoparticle diameter.

noticeably influenced by the extra term that appears in the energy equation due to Brownian diffusion.

Comparisons of convective heat transfer coefficient ratio of nanofluid and base fluid with Peclet number for 2% volume fraction of Al_2O_3-water nanofluid have been shown in Fig. 12 which shows almost similar results for different models. Mixture-phase model exhibits slightly lower values of convective heat transfer coefficient ratio than Heris et al. [60] and single-phase models but the variation is so small that it is acceptable. For all the models, a tendency of increment of convective heat transfer coefficient has been identified with the increment of Peclet number.

Efficiency of flat plate solar collector for various volume fraction of Al_2O_3-water nanofluid at a constant flow rate of 0.02 mL/s has been shown in Figure 13 which shows a significant increment of efficiency by utilizing volume fraction of Al_2O_3-water nanofluid. Around 6.5% and 6.2% increment of efficiency than base fluid has been observed for single-phase and mixture-phase model respectively by utilizing 5% volume fraction of nanoparticle. Mixture-phase model gives slightly lower value of efficiency than single-phase model due to the lower value of convective heat transfer coefficient.

Efficiency of flat plate solar collector for various volume fraction of Al_2O_3-water nanofluid at a constant flow rate of 0.03 mL/s and 0.04 mL/s have been shown in Figure 14 and Figure 15 respectively which also exhibit significant increment of efficiency by utilizing volume fraction of

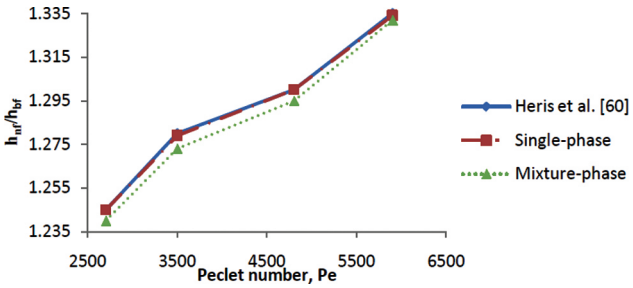

Figure 12. Comparison of convective heat transfer coefficient ratio of nanofluid and base fluid with Peclet number for 2% volume fraction of Al_2O_3-water nanofluid.

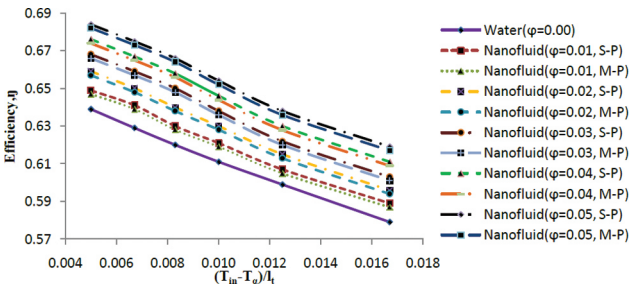

Figure 13. Efficiency of flat plate collector for various volume fractions of Al_2O_3-water nanofluid at Q=0.02 mL/s.

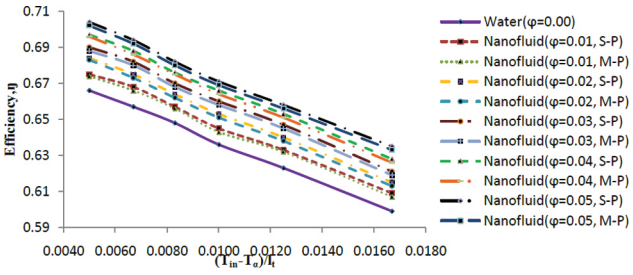

Figure 14. Efficiency of flat plate collector for various volume fractions of Al_2O_3-water nanofluid at Q=0.03 mL/s.

Al_2O_3-water nanofluid. Efficiency increment reduces with the increment of flow rate. Around 5.7% and 5.4% increment of efficiency than base fluid have been observed for single-phase and mixture-phase model respectively by utilizing 5% volume fraction of nanoparticle for flow rate of 0.03 mL/s whereas the increment is 4.95% and 4.7% for single-phase and mixture-phase model respectively for flow rate of 0.04 mL/s.

Efficiency of flat plate solar collector for various volume fractions of Al_2O_3-water nanofluid at different flow rates has been shown in Figure 16. Here, $(T_{in}-T_{\alpha})/I_t$ has been considered 0.005. It can be clearly visible from the figure that

efficiency increases not only with the increment of volume fraction of nanofluid but also with the increment of flow rates whenever the valaue of value of $(T_{in}-T_{\alpha})/l_t$ is constant.

Efficiency of flat plate solar collector for various volume fraction of CuO-water nanofluid at a constant flow rate of 0.03 mL/s has been shown in Figure 17 which shows comparatively more increment of efficiency by utilizing volume fraction of CuO-water nanofluid. Nearly 8.7% increment of efficiency than base fluid has been observed for single-phase model by utilizing 5% volume fraction of nanoparticle. So, CuO-water nanofluid provides 2% more efficiency than utilizing Al_2O_3-water nanofluid.

Efficiency of flat plate solar collector with variable overall heat loss coefficient for various volume fraction of Al_2O_3-water and CuO-water nanofluid has been shown in Figure 18 and Figure 19 respectively which also exhibit significant increment of efficiency by utilizing volume fraction of nanofluid. For 5% volume fraction of nanoparticle, about 4.9% and 7.1% increment of efficiency than base fluid have been observed for Al_2O_3-water and CuO-water nanofluid respectively. So, CuO-water nanofluid provides 2.2% more efficiency than utilizing Al_2O_3-water nanofluid.

Efficiency of flat plate solar collector by utilizing internal fins to the riser tubes at a constant flow rate of 0.03 mL/s has been shown in Figure 20 which shows noticeable increment of efficiency for utilizing fins to the riser tubes. Up to 2% and 11% increment of efficiency has been observed for fin-1 and fin-2 respectively.

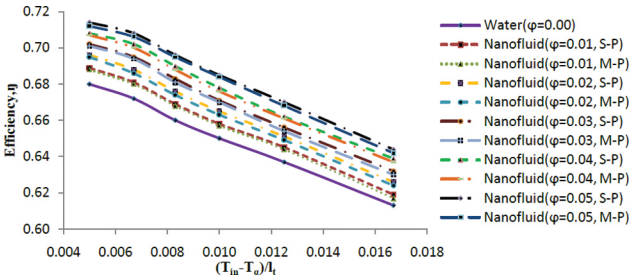

Figure 15. Efficiency of flat plate collector for various volume fractions of Al_2O_3-water nanofluid at Q=0.04 mL/s.

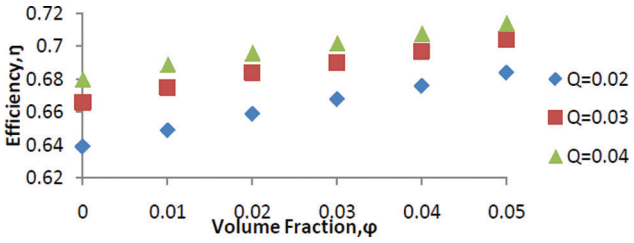

Figure 16. Efficiency of flat plate collector for various volume fractions of Al_2O_3-water nanofluid at different flow rates (Considering, $(T_{in}-T_{\alpha})/l_t = 0.005$).

CONCLUSION

It has been observed that average convective heat transfer coefficient and average shear stress have been increased up to 36% and 196% respectively by increasing volume fraction of nanoparticle. A significant increment of average

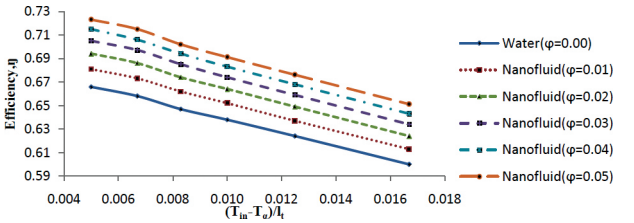

Figure 17. Efficiency of flat plate collector for various volume fractions of CuO-water nanofluid at Q=0.03 mL/s.

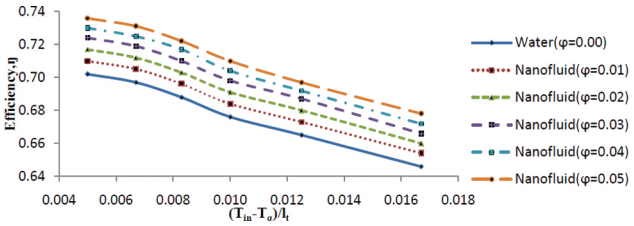

Figure 18. Efficiency of flat plate collector for various volume fractions of Al_2O_3-water nanofluid with variable U_L.

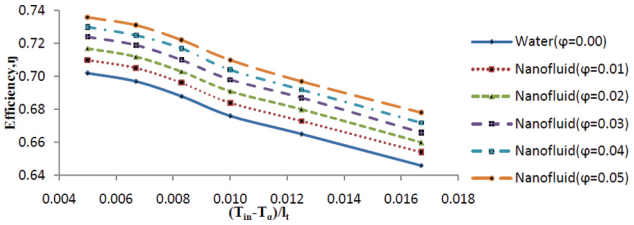

Figure 19. Efficiency of flat plate collector for various volume fractions of CuO-water nanofluid with variable U_L.

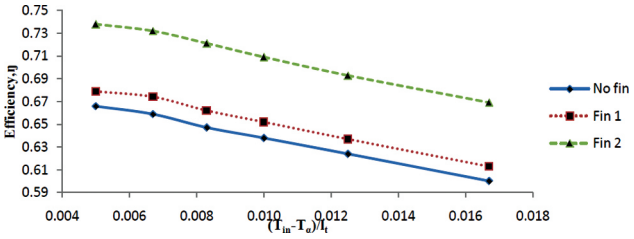

Figure 20. Efficiency of flat plate collector for utilizing internal fins to the riser tubes.

Nusselt number has been found by increasing Reynolds number but Nusselt number is slightly affected by the increment of volume fraction of nanoparticle. Mixture-phase model gives fewer values of average convective heat transfer coefficient, average Nusselt number, average shear stress and efficiency in comparison to single-phase model due to the reduction of viscosity near the wall. Sensitivity of particle diameter has been observed in case of mixture phase model. The extra term that appears in the energy equation of mixture phase model because of Brownian diffusion has not significantly influenced the heat transfer coefficient.

Increment of efficiency of flat plate collector has been observed with the increment of volume fraction of nanoparticle. However, the increment is comparatively lower for higher flow rates in comparison to the base fluid. Utilizing CuO-water nanofluid gives higher efficiency than Al_2O_3-water nanofluid. Efficiency has been increased up to 6.5% and 8.7% than the base fluid by utilizing Al_2O_3-water and CuO-water nanofluid respectively in case of constant heat loss coefficient. Noticeable increment of efficiency has been observed for variable overall heat loss coefficient from the constant heat loss coefficient but this time, increment percentage is lower from the base fluid for utilizing nanofluid. The reason behind this is the higher amount of constant heat loss coefficient (8 W/m^2K) in comparison to the variable overall heat loss coefficient. Efficiency has been increased up to 4.9% and 7.1% than the base fluid by utilizing Al_2O_3-water and CuO-water nanofluid respectively. The efficiency has been improved up 2% by utilizing fin-1 but the efficiency has been increased up to 11% in comparison to the no fin case by utilizing fin-2. So, utilizing internal fins give the highest efficiency of flat plate solar collector which can be used for various purposes. For improving the performance of solar collector, further researches can be made utilizing other types of fin arrangements, other types of nanofluids and other types of solar collectors which can be compared with this study.

NOMENCLATURE

A_c	Absorber plate's surface area [m^2]
T_p	Absorber plate's temperature [°C or K]
T_α	Ambient temperature [°C or K]
z	Axial location
f	Body forces [N]
D_B	Brownian diffusion coefficient
h	Convective heat transfer coefficient [$Wm^{-2}K^{-1}$]
D	Diameter [m]
u	Flow velocity vector [m/s]
m	Mass flow rate [kg/s]
V_o	Normal inflow velocity [m/s]
Nu	Nusselt number
U_L	Overall heat loss coefficient
Pe	Peclet number
Pr	Prandtl number
p	Pressure [Pa]
R	Radial location
r	Radius [m]
Re	Reynolds number
I_t	Solar irradiation
S	Source term
T	Temperature [°C or K]
k	Thermal conductivity [$Wm^{-1}K^{-1}$]
D_T	Thermophoretic diffusion coefficient
L	Total length [m]
V	Velocity [m/s]

Greek letter

$\cdot$	Density
μ	Dynamic viscosity
η	Efficiency
φ	Nanoparticle volume fraction
$\tau\alpha$	Solar plate's total absorption coefficient
α	Thermal diffusivity
τ_s	Wall shear stress

Subscript

av	Average
z	Axial direction
bf	Basefluid
b	Bottom
e	Edge
in	Inlet
nf	Nanofluid
np	Nanoparticle
out	Outlet
r	Radial direction
t	Top

AUTHORSHIP CONTRIBUTIONS

Concept: Farzad Hossain; Design: Farzad Hossain; Supervision: Eric Hu; Materials: Farzad Hossain, Md. Ashrafuzzaman Miah; Data: Farzad Hossain, Md. Ashrafuzzaman Miah, Afshana Morshed, Md Insiat Islam Rabby; Analysis: Farzad Hossain, Md. Ashrafuzzaman Miah, Afshana Morshed, Md Insiat Islam Rabby; Literature search: Farzad Hossain, Md. Ashrafuzzaman Miah, Afshana Morshed, Md Insiat Islam Rabby; Writing: Farzad Hossain, Md. Ashrafuzzaman Miah, Afshana Morshed, Md Insiat Islam Rabby; Critical revision: Farzad Hossain, Md. Ashrafuzzaman Miah, Eric Hu

REFERENCES

[1] Ahmed MS. Nanofluid: New Fluids by Nanotechnology. In: Shahzad A, editor. Thermophysical Properties of Complex Materials. London: IntechOpen; 2019: 1-17.

[2] Choi SUS, Eastman JA. Enhancing thermal conductivity of fluids with nanoparticles. Illinois, United States: Argonne National Lab.; 1995.
[3] Agarwal DK, Vaidyanathan A, Kumar SS. Synthesis and characterization of kerosene–alumina nanofluids. Appl Therm Eng 2013;60:275-284. [CrossRef]
[4] Liu L, Stetsyuk V, Kubiak KJ, Yap YF, Goharzadeh A, Chai JC. Nanoparticles for convective heat transfer enhancement: Heat transfer coefficient and the effects of particle size and zeta potential. Chem Eng Commun 2019;206:761-771. [CrossRef]
[5] Sridhara V, Satapathy LN. Al_2O_3-based nanofluids: a review. Nanoscale Res Lett 2011;6:456.
[6] Mahbubul IM, Saidur R, Amalina MA. Latest developments on the viscosity of nanofluids. Int J Heat Mass Transf 2012;55:874-885. [CrossRef]
[7] Abbasi S, Zebarjad SM, Baghban SHN, Youssefi A. Statistical analysis of thermal conductivity of nanofluid containing decorated multi-walled carbon nanotubes with TiO_2 nanoparticles. Bull Mater Sci 2014;37:1439-1445. [CrossRef]
[8] Davarnejad R, Barati S, Kooshki M. CFD simulation of the effect of particle size on the nanofluids convective heat transfer in the developed region in a circular tube. Springer Plus 2013;2:1-6. [CrossRef]
[9] Rabby MI, Hossain F, Amin SS, Islam AS. Numerical simulation on performance evaluation among metal and oxide based nanofluids for power savings application of a circular tube. J Therm Eng 2021;7:1150-1162. [CrossRef]
[10] Rabby MI, Hossain F, Amin SS, Mumu TA, Bhuiyan MA, Islam AS. Convective heat transfer and power saving application of si based nanoparticles in a circular pipe. Lat Am Appl Res 2020;50:321-327. [CrossRef]
[11] Hossain F, Miah MA. Utilization of Organic Rankine Cycle for Analyzing Energy and Exergy of the Waste Heat Recovery System. Sigma J Eng Nat Sci 2020;38:1963-1976.
[12] Verma SK, Sharma K, Gupta NK, Soni P, Upadhyay N. Performance comparison of innovative spiral shaped solar collector design with conventional flat plate solar collector. Energy 2020;194:116853. [CrossRef]
[13] Manjunath MS, Karanth VK, Sharma YN. Three dimensional numerical analysis of conjugate heat transfer for enhancement of thermal performance using finned tubes in an economical unglazed solar flat plate collector. Proceedings of the World Congress on Engineering, London: 2011. p. 2245-2249.
[14] Rassamakin B, Khairnasov S, Zaripov V, Rassamakin A, Alforova O. Aluminum heat pipes applied in solar collectors. Sol Energy 2013;94:145-154.
[15] Chaji H, Ajabshirchi Y, Esmaeilzadeh E, Heris SZ, Hedayatizadeh M, Kahani M. Experimental study on thermal efficiency of flat plate solar collector using TiO_2/water nanofluid, Mod Appl Sci 2013;7:60-69. [CrossRef]
[16] Nasrin R, Alim MA. Finite element simulation of forced convection in a flat plate solar collector: influence of nanofluid with double nanoparticles. J Appl Fluid Mech 2014;7:543-556. [CrossRef]
[17] Tiwari GN, Yadav JK, Singh DB, Al-Helal IM, Abdel-Ghany AM. Exergoeconomic and enviroeconomic analyses of partially covered photovoltaic flat plate collector active solar distillation system. Desalination 2015;367:186-196. [CrossRef]
[18] Verma SK, Tiwari AK, Chauhan DS. Experimental evaluation of flat plate solar collector using nanofluids. Energy Convers Manag 2017;134:103-115. [CrossRef]
[19] Genc AM, Ezan MA, Turgut A. Thermal performance of a nanofluid-based flat plate solar collector: A transient numerical study. Appl Therm Eng 2018;130:395-407. [CrossRef]
[20] Hawwash AA, Rahman AKA, Nada SA, Ookawara S. Numerical investigation and experimental verification of performance enhancement of flat plate solar collector using nanofluids. Appl Therm Eng 2018;130:363-374. [CrossRef]
[21] Mahbubul IM, Khan MMA, Ibrahim NI, Ali HM, Al-Sulaiman FA, Saidur RJRE. Carbon nanotube nanofluid in enhancing the efficiency of evacuated tube solar collector. Renewable energy 2018;121:36-44. [CrossRef]
[22] Kiliç F, Menlik T, Sözen A. Effect of titanium dioxide/water nanofluid use on thermal performance of the flat plate solar collector. Sol Energy 2018;164:101-108. [CrossRef]
[23] Khan MMA, Ibrahim NI, Mahbubul IM, Ali HM, Saidur R, Al-Sulaiman FA. Evaluation of solar collector designs with integrated latent heat thermal energy storage: a review. Sol Energy 2018;166:334-350. [CrossRef]
[24] Pandey KM, Chaurasiya R. A review on analysis and development of solar flat plate collector. Renew Sust Energy Rev 2017;67:641-650. [CrossRef]
[25] Hussein AK. Applications of nanotechnology in renewable energies-A comprehensive overview and understanding, Renew Sust Energy Rev 2015;42:460-476. [CrossRef]
[26] Hussein AK, Walunj A, Kolsi L. Applications of nanotechnology to enhance the performance of the direct absorption solar collectors. J Therm Eng 2016;2:529-540. [CrossRef]
[27] Li D, Li Z, Zheng Y, Liu C, Hussein AK, Liu X. Thermal performance of a PCM-filled double-glazing unit

with different thermophysical parameters of PCM. Sol Energy 2016;133:207-220. [CrossRef]
[28] Hussein AK. Applications of nanotechnology to improve the performance of solar collectors – Recent advances and overview. Renew Sust Energy Rev 2016;62:767-792. [CrossRef]
[29] Hussein AK, Li D, Kolsi L, Kata S, Sahoo B. A review of nano fluid role to improve the performance of the heat pipe solar collectors. Energy Procedia 2007;109:417-424. [CrossRef]
[30] Chand R, Rana G, Hussein AK. On the onset of thermal instability in a low Prandtl number nanofluid layer in a porous medium. JAppl Fluid Mech 2015;8:265-272. [CrossRef]
[31] Kareem AK, Mohammed HA, Hussein AK, Gao S. Numerical investigation of mixed convection heat transfer of nanofluids in a lid-driven trapezoidal cavity. Int Commun Heat Mass Transf 2016;77:195-205. [CrossRef]
[32] Kamel M, Lezsovits F, Hussein AK. Experimental studies of flow boiling heat transfer by using nanofluids : a critical recent review. J Therm Anal Calorim 2019;138:4019-4043. [CrossRef]
[33] Al-Rashed AA, Kalidasan K, Kolsi L, Velkennedy R, Aydi A, Hussein AK, et al. Mixed convection and entropy generation in a nanofluid filled cubical open cavity with a central isothermal block. Int J Mech Sci 2018;135:362-375. [CrossRef]
[34] Mehryan SAM, Alsabery A, Modir A, Izadpanahi E, Ghalambaz M. Fluid-structure interaction of a hot flexible thin plate inside an enclosure. Int J Therm Sci 2020;153:106340. [CrossRef]
[35] Yarmohammadi S, Mohammadzadeh K, Farhadi M, Hajimiri H, Modir A. Multi-objective optimization of thermal and flow characteristics of R-404A evaporation through corrugated tubes. J Energy Storage 2020;27:101137.
[36] Zayed ME, Zhao J, Du Y, Kabeel AE, Shalaby SM. Factors affecting the thermal performance of the flat plate solar collector using nanofluids: a review. Sol Energy 2019;182:382-396. [CrossRef]
[37] Saffarian MR, Moravej M, Doranehgard MH. Heat transfer enhancement in a flat plate solar collector with different flow path shapes using nanofluid. Renew Energy 2020;146:2316-2329. [CrossRef]
[38] Sharafeldin MA, Gróf G. Experimental investigation of flat plate solar collector using CeO_2-water nanofluid. Energy Convers Manag 2018;155:32-41. [CrossRef]
[39] Jouybari HJ, Saedodin S, Zamzamian A, Nimvari ME, Wongwises S. Effects of porous material and nanoparticles on the thermal performance of a flat plate solar collector: an experimental study. Renew Energy 2017;114:1407-1418. [CrossRef]
[40] Farshad SA, Sheikholeslami M, Hosseini SH, Shafee A, Li Z. Nanofluid turbulent forced convection through a solar flat plate collector with Al_2O_3 nanoparticles. Microsyst Technol 2019;25:4237-4247. [CrossRef]
[41] Akram N, Sadri R, Kazi SN, Zubir MNM, Ridha M, Ahmed W, et al. A comprehensive review on nanofluid operated solar flat plate collectors. J Therm Anal Calorim 2020;139:1309-1343. [CrossRef]
[42] Tong Y, Lee H, Kang W, Cho H. Energy and exergy comparison of a flat-plate solar collector using water, Al_2O_3 nanofluid, and CuO nanofluid. Appl Therm Eng 2019;159:113959. [CrossRef]
[43] Kundu B. Thermal analysis on variable thickness absorber plate fin in flat-plate solar collectors using differential transform method. J Therm Eng 2020;6:157-169. [CrossRef]
[44] Roy S, Asirvatham LG, Kunhappan D, Cephas E, Wongwises S. Heat transfer performance of silver/water nanofluid in a solar flat-plate collector. J Therm Eng 2015;1:104-12. [CrossRef]
[45] Batchelor GK. An Introduction to Fluid Dynamics. Cambridge University Press: Cambridge; 1967.
[46] Cengel YA. Fluid mechanics. New York: Tata McGraw-Hill Education; 2010.
[47] Buongiorno J. Convective transport in nanofluids. J Heat Transf 2006;128:240. [CrossRef]
[48] Gerhart PM, Gerhart AL, Hochstein JI. Munson, Young and Okiishi's fundamentals of fluid mechanics. John New Jersey: Wiley & Sons; 2016.
[49] Vafai K. Handbook of porous media. New York: CRC Press; 2015. [CrossRef]
[50] Mackowski DW. Conduction heat transfer: Notes for MECH 7210. Mechanical Engineering Department, Auburn University, 2011.
[51] Hossein A, Farahat S, Sarhaddi F. Exergetic Optimization of Solar Air Heaters and Comparison with Energy Analysis. Int J Thermodyn 2005;8:183-190.
[52] Cengel Y. Heat and mass transfer: fundamentals and applications. New York: McGraw-Hill Higher Education; 2014.
[53] Struckmann F. Analysis of a flat-plate solar collector. Heat and Mass Transport, Project Report, 2008MVK160, 2008.
[54] Nguyen CT, Desgranges F, Roy G, Galanis N, Maré T, Boucher S, et al. Temperature and particle-size dependent viscosity data for water-based nanofluids–hysteresis phenomenon. Int J Heat Fluid Flow 2007;28:1492-1506. [CrossRef]
[55] Pak BC, Cho YI. Hydrodynamic and heat transfer study of dispersed fluids with submicron metallic oxide particles. Exp Heat Transf Int J 1998;11:151-170. [CrossRef]

[56] Eastman JA, Choi U, Li S, Thompson LJ, Lee S. Enhanced thermal conductivity through the development of nanofluids. MRS Online Proceedings Library Archive. 1996;457:3-12. [CrossRef]

[57] Xuan Y, Li Q. Heat transfer enhancement of nanofluids. Int J Heat Fluid Flow 2000;21:58-64. [CrossRef]

[58] Shah RK, London AL. Laminar Forced Convection in Ducts. Advances in Heat Transfer. New York: Academic Press; 1978.

[59] Kalogirou SA. Solar thermal collectors and applications. Progr Energy Combust Sci 2004;30:231-295. [CrossRef]

[60] Heris SZ, Esfahany MN, Etemad SG. Experimental investigation of convective heat transfer of Al_2O_3/water nanofluid in circular tube. Int J Heat Fluid Flow 2007;28:20310. [CrossRef]